EUROPEAN ACADEMIC RESEARCH
Vol. VI, Issue 5/ August 2018

Impact Factor: 3.4546 (UIF)
DRJI Value: 5.9 (B+)

ISSN 2286-4822
www.euacademic.org

Application of Response Surface and Factorial Regression Models in Estimating Global Solar Radiation and Ultraviolet Index

GHADA I. EL-SHANSHOURY
Radiation Safety Department
Nuclear and Radiological Regulatory Authority (NRRA)
Cairo, Egypt

Abstract:

This study is intended to develop predictive models for estimating monthly and daily clear sky global solar radiation on a horizontal surface ($\bar{H}$) *and maximum ultraviolet index* (UVI_{max}) *for some cities in Egypt. Choosing the preferred model depends on the best and most accurate results. The applicable empirical regression models are confined in multiple linear regression model, factorial regression model and response surface regression model. The investigated models are applied for forecasting daily and monthly clear sky global solar radiation and maximum UVI for cities of Sharm El-Sheikh, Aswan, Safaga and Cairo. The new developing predictive models are calibrated. The regression models for estimating global solar radiation are based on three major predictor variables and their interactions. The predictor variables are cosine solar zenith angle at mid-time between sunrise and solar noon* ($\cos(\theta_{ZMT})$), *average air temperature* ($\bar{T}$) *and maximum possible sunshine duration* (S_0). *The developed empirical models are considered as a simplified statistical approach for daily estimation of* $\bar{H}$ *because they depend on two monthly constant parameters* (S_0 & $\cos(\theta_{ZMT})$) *and one daily changeable parameter* ($\bar{T}$). *Precision of* UVI_{max} *forecasting models is based on two parameters, which are accurate prediction results of clear sky global solar radiation and maximum temperature. Some statistical performance indicators measure the results accuracy of empirical*

predictive models. The results of the developed models show that the factorial regression models and the response surface regression models give more precised results than the multiple linear regression models. The predicted results of global solar radiation and maximum ultraviolet index overlap the measured data in all months of the year.

Key words: Ultraviolet index, Clear sky global solar radiation, Cosine solar zenith angle, Air temperature and Maximum possible sunshine duration.

1. INTRODUCTION

Ultraviolet (*UV*) radiation is a form of electromagnetic radiation. The main source of *UV* radiation (rays) is the sun, although it can also come from man-made sources such as tanning beds and welding torches (American Cancer Society). Ionizing radiation is made up of energetic subatomic particles, ions or atoms moving at high speeds, and electromagnetic waves on the high-energy end of the electromagnetic spectrum. Gamma rays, X-rays, and the higher ultraviolet part of the electromagnetic spectrum are ionizing (Wikipedia, ionizing radiation). Higher energy *UV* rays often have enough energy to remove an electron from (ionize) an atom or molecule, making them a form of ionizing radiation (American Cancer Society), whereas the lower ultraviolet part of the electromagnetic spectrum and all the spectrum below *UV*, including visible light (including nearly all types of laserlight), infrared, microwaves, and radio waves are considered non-ionizing radiation (Wikipedia, ionizing radiation).

Solar radiation is an important natural factor because it forms the Earth's climate and has a significant effectiveness on the environment. Solar radiation is radiant energy that emitted by the sun from a nuclear fusion reaction that creates electromagnetic energy. About half of the radiation is in the visible short-wave part of the electromagnetic spectrum. The other half is mostly in the near-infrared part, with some in the ultraviolet part of the spectrum (AmbientWeather). The estimation of global solar radiation is necessary for utilization the solar energy, design when proper

observation values are missing. The values of solar radiation in clear skies are useful for determination of the maximum performance heating and photovoltaic, moreover, for the design of air conditioning equipment in buildings or for the determination of thermal load their solar installations (El Mghouchi et al 2014).

The ultraviolet is a part of the solar spectrum (*UV*) that plays an important role in many processes in the biosphere. It has several beneficial influence but it may also be very harmful if UV exceeds "safe" levels. If the amount of *UV* radiation is enough high the self-protection ability of some biological kinds is exhausted and the subject may be severely damaged. This is also concerned to the human organism, in specific the skin and the eyes. To avoid the harm from high UV exposures, people should limit their exposure to solar radiation by using protective procedures. The need to reach the public with simple-to-understand information about *UV* and its possible hazardous effects led scientists to define a parameter that can be used as an indicator of the *UV* exposures. This parameter is called the *UV* Index (*UVI*). It is associated to the erythemal effects of solar *UV* radiation on human skin (Vanicek et al 1999).

The *UV* Dose (*UVD*) is directly associated to some health effect on humans. A 50% increase in erythemal *UVD* would consequently increase the rate at which the skin reddens by 50% (Wiegant et al. 2016). However, Hatfield et al., (2009) found statistical relations between exceedance of threshold *UVI* values and cancer incidence rates by investigating the relation between *UV* exposure and non-melanoma skin cancer using a statistical model. On the other hand, the acute effects of radiation exposure on skin are well known and result in severe skin burns. As well as, low levels of ionizing radiation to skin have been observed as well. The accompanying erythema, which resembled a burn, was painless; but, chronic radiation dermatitis following repeated exposure is usually extremely painful. Five progressive categories of radiation damage are observed in skin: (1) erythema, (2) transepithelial injury (moist desquamation), (3) ulceration, (4) necrosis, and (5) skin cancer (Miller et al., in press). The *UVI* is now widely used in many operational weather reports and forecasts. In Europe, for example, there are more than a dozen forecasting centers that release estimated *UVI* values for countries or regional areas. Different methods are used to predict the *UVI* .

Operational *UVI* forecasting has already been executed in many countries. The forecast methods vary from simple statistical methods has utilized for local areas to more complicated methods with global coverage and with forecast times from a few hours to several days, either for clear sky or all sky conditions (Vanicek et al 1999).

Several researchers have developed statistical models to predict monthly global solar radiation on a horizontal surface $(\bar{H})$ using multiple linear regression equations with different independent variables (predictor variables). Some of these predictors (weather parameters) are represented in, mean relative sunshine duration (S/S_0), mean daily maximum temperature (T_{max}), mean daily relative humidity (Rh), mean daily rainfall (R), mean daily temperature ($\bar{T}$), ratio of maximum and minimum daily temperature and other weather parameters (Falayi et al 2008, Augustine and Nnabuchi 2009, Habbib 2011, Ituen et al 2012 , Chen and Li 2012, Adhikari et al 2013, Namrata et al 2016).

El-shanshoury et al (2017), developed the model with multiple regression equation for Sharm El-Sheikh city. This model differs from other searchers empirical models that predict the monthly clear sky monthly global solar radiation future time $(\bar{H})$. The developed multiple linear regression model is based on three predictor parameters as independent variables. These parameters are: monthly average cosine solar zenith angle at mid-time between sunrise and solar noon $\cos(\theta_{ZMT})$, monthly average daily mean temperature (T) and monthly average day length (S_0). Two predictors are calculated (S_0 & $\cos(\theta_{ZMT})$) and one predictor is measured (T). This model is considered as a simplified statistical approach for daily estimation of $\bar{H}$ because it depends on two monthly constant predictors (S_0 & $\cos(\theta_{ZMT})$) and one daily changeable predictor ($\bar{T}$). The developing models for estimating global solar radiation data, using commonly and available meteorological records such as temperature, are calibrated. The results of our previous work deduced that the uses of the above mentioned predictors reduce error rate nearly by 40-50% when compared with other searchers developed models. As well as, UVI_{max} is modeled for forecasting its monthly and daily value. The

statistical prediction UVI_{max} model is based on two independent variables for constructing the multiple linear regression equation. The first predictor is the monthly mean daily clear sky global solar radiation on a horizontal surface $(\bar{H})$ and the second predictor is monthly average maximum temperature ($\bar{T}_{\max}$). After trying many weather parameters for modeling UVI_{max}, The model's predictors found more parameters that are accurate for UVI_{max} forecasting results than other parameters.

In this work new developed models are utilized with the same parameters of our previous work for estimating $\bar{H}$ and UVI_{max}. The regression models are restricted in multiple linear regression model, factorial regression model and response surface regression model.

2. MATERIALS AND METHODS

The material data of monthly averaged clear sky global radiation on a horizontal surface ($\bar{H}$ in kWh/m^2/day) and monthly average air mean and maximum temperature at 10m above the earth (T & T_{max} in degrees celsius) is obtained from NASA meteorology (NASA). The data covered a period of 22 years (1983 – 2005) for Sharm El-Shiekh, Aswan Safaga and Cairo in Egypt. The latitude and longitude for Sharm El-Shiekh are 27.912^o and 34.33^o, respectively, for Aswan are 24.0908°and 32.8994°, for Safaga are 26.7453° and 33.95059°, and for Cairo are 30.06263° and 31.24967°. Maximum *UVI* data is obtained from weather2travel-climate guides (weather2travel).

In this work five developed models are utilized and compared using the same our previous work parameters (T, $\cos(\theta_{\mathrm{ZMT}})$ and S_0) with different techniques. These models are applied for estimating monthly and daily clear sky global solar radiation on a horizontal surface $(\bar{H}$ and H, respectively$)$. As well as, three developed models are used for estimating monthly and daily UVI_{max} by using two parameters ($\bar{H}$ or H and T_{max}). The regression models are multiple linear regression model, factorial regression model and response surface regression model.

Multiple regression designs are restricted to continuous predictor (independent) variables, as main effect ANOVA designs are to categorical predictor variables. Multiple regression designs contain the separate simple regression designs for 2 or more continuous predictor variables. The regression equation for a multiple regression design for the first-order effects includes 3 continuous predictor variables *C*, *T* and *S* is

$$Y = b_0 + b_1C + b_2T + b_3S$$ (Hill and Lewicki 2007).

Factorial regression designs are similar to factorial ANOVA designs, in which amalgamation of the levels of the factors are represented in the design. In factorial regression designs, there may be many more such possible combinations of distinct levels for the continuous independent variables than there are cases in the data set. That is, full-factorial regression designs are defined as designs in which all possible products of the continuous predictor variables are represented in the design. For example, the full-factorial regression design for two continuous predictor variables *C* and *T* will include the main effects (i.e., the first-order effects) of *C* and *T* and their 2-way *C* by *T* interaction effect, which is represented by the product of *C* and *T* scores for each case. The regression equation is $Y = b_0 + b_1C + b_2T + b_3C*T$. Factorial regression designs can also be fractional, that is, higher-order effects can be omitted from the design. A fractional design for 3 continuous predictor variables *C*, *T* and *S* will include the main effects and all 2-way interactions between the predictor variables is

$Y = b_0 + b_1C + b_2T + b_3S + b_4C*T + b_5C*S + b_6T*S$ (Hill and Lewicki 2007).

Response surface regression Quadratic response surface regression designs are a hybrid type of design with characteristics of both polynomial regression designs and fractional factorial regression designs. Quadratic response surface regression designs contain all the same effects of polynomial regression designs to degree 2 (second order), and additionally the 2-way interaction effects of the predictor variables. The regression equation for a quadratic response surface regression design for 2 continuous predictor variables *C, T* is $Y = b_0 + b_1C + b_2C^2 + b_3T + b_4T^2 + b_5C*T$. As well as, 3 continuous predictor variables *C*, *T* and *S* is

$Y = b_0 + b_1C + b_2C^2 + b_3T + b_4T^2 + b_5S + b_6S^2 + b_7C*T + b_8C*S + b_9T*S$ (Hill and Lewicki 2007).

The suggested modified empirical model of clear sky global solar radiation has been estimated on the basis of measurements of monthly averaged clear sky global radiation on a horizontal surface and monthly average air mean temperature for under investigation states. Also, the empirical model is based on calculation of monthly mean daily extraterrestrial radiation and monthly average cosine solar zenith angle at mid-time between sunrise and solar noon and maximum possible sunshine duration for each state.

2.1. Empirical regression models to estimate monthly average daily clear sky global radiation $(\bar{H})$

The devolved regression models for estimating $\bar{H}$ are based on three major predictor variables and their interactions. The major predictor parameters are $\cos(\theta_{ZMT})$, T and S_0 . The response variable is monthly averaged clear sky insolation clearness index that calculated to be predictable of $\bar{H}$. Five empirical models are applied to estimate the monthly and daily average clear sky global radiation. $\bar{H}$ is modeled as follow:

2.1.1. Predictive Multiple Linear Regression (MLR) model

The first-order regression model for three continuous predictor variables (C, T and S) takes the form

Model 1:

$$\frac{\bar{H}}{\bar{H}_0} = b_0 + b_1C + b_2T + b_3S \qquad (1)$$

$$\bar{H}_{estimated} = (b_0 + b_1C + b_2T + b_3S)* \bar{H}_0 \qquad (2)$$

2.1.2. Predictive Factorial Regression (FR) model

The interaction regression model for two continuous predictor variables (C and T) takes the form

Model 2:

$$\frac{\bar{H}}{\bar{H}_0} = b_0 + b_1C + b_2T + b_3C*T \quad (3)$$

$$\bar{H}_{estimated} = (b_0 + b_1C + b_2T + b_3C*T)* \bar{H}_0 \quad (4)$$

The interaction regression model for three continuous predictor variables (*C, T* and *S*) takes the form

Model 3:

$$\frac{\bar{H}}{\bar{H}_0} = b_0 + b_1C + b_2T + b_3S + b_4C*T + b_5C*S + b_6T*S \quad (5)$$

$$\bar{H}_{estimated} = (b_0 + b_1C + b_2T + b_3S + b_4C*T + b_5C*S + b_6T*S)* \bar{H}_0 \quad (6)$$

2.1.3. Predictive Response Surface Regression (RSR) model

The second-order polynomial regression model for two continuous predictor variables (*C* and *T*) takes the form

Model 4:

$$\frac{\bar{H}}{\bar{H}_0} = b_0 + b_1C + b_2C^2 + b_3T + b_4T^2 + b_5C*T \quad (7)$$

$$\bar{H}_{estimated} = (b_0 + b_1C + b_2C^2 + b_3T + b_4T^2 + b_5C*T)* \bar{H}_0 \quad (8)$$

The second-order polynomial regression model for three continuous predictor variables (*C, T* and *S*) takes the form

Model 5:

$$\frac{\bar{H}}{\bar{H}_0} = b_0 + b_1C + b_2C^2 + b_3T + b_4T^2 + b_5S + b_6S^2 + b_7C*T + b_8C*S + b_9T*S \quad (9)$$

$$\bar{H}_{estimated} = (b_0 + b_1C + b_2C^2 + b_3T + b_4T^2 + b_5S + b_6S^2 + b_7C*T + b_8C*S + b_9T*S)* \bar{H}_0 \quad (10)$$

Where, *b's* are the coefficients of predictor variables, $\bar{H}/\bar{H}_0$ is monthly average clear sky insolation clearness index, $\bar{H}$ is the measure of monthly mean daily clear sky global solar radiation on a horizontal surface, $\bar{H}_0$ is monthly mean daily extraterrestrial radiation KW/m^2, *C* represents monthly average cosine solar zenith angle at mid-time

between sunrise and solar noon $\cos(\theta_{ZMT})$, T represents monthly average daily mean temperature , S represents monthly average day length (S_0) and $\overline{T}$ is daily mean temperature.

The values of the monthly average daily extraterrestrial radiation ($\overline{H}_0$) can be calculated from the following equation (Duffie and Beckman 2013).

$$\overline{H}_0 = \frac{24}{\pi} I_{SC} E_0 \left[\cos\phi \cos\delta \sin w_s + \frac{\pi w_s}{180} \sin\phi \sin\delta \right] \quad (11)$$

$$E_0 = 1 + 0.033 \cos\left[\frac{360 d_n}{365} \right]$$

where, I_{SC} is the solar constant (=1.367 KWm^{-2}), ϕ is the latitude of the site, δ is the solar declination, w_s is the mean sunrise hour angle for the given month, and d_n is the number of days of the year starting from the first of January (the Julian day number) .

The solar declination (δ) and the mean sunrise hour angle (w_s) can be calculated by the following equations:

$$\delta = 23.45 \sin\left[360 \frac{(d_n + 284)}{365} \right] ,$$

$$w_s = \cos^{-1}\left(-\tan\phi \tan\delta \right)$$

The maximum possible sunshine duration (S_0) (or monthly average day length) which is related to w_s, can be computed by using the following equation:

$$S_0 = \frac{2}{15} w_s \quad (12)$$

Monthly average cosine solar zenith angle at mid-time between sunrise and solar noon is calculated according the following formula (NASA).

$\cos(\theta_{ZMT}) = f + g[(g - f) / 2g]^{½}$ (13)

where, $f = \sin(\phi)\sin(\delta)$, $g = \cos(\phi)\cos(\delta)$

Average daily mean temperature ($\overline{T}$) is calculated as follows:

$$\overline{T} = \frac{(T_{\max imum} + T_{\min imum})}{2} \quad (14)$$

The estimated daily estimating daily clear sky global solar radiation on a horizontal surface (H) is derived from monthly $\overline{H}$ estimation model.

2.2. Empirical regression models to estimate the monthly maximum ultraviolet index (UVI_{max})

The statistical forecasting models for estimation of monthly average maximum ultraviolet index are based on two parameters to construct the regression models. The first parameter is $\overline{H}_{estimated}$ and the second parameter is $\overline{T}_{\max}$. Models 6-8 present the investigated forecasting models.

2.2.1. Predictive multiple linear regression model

Model 6:

$$UVI_{max} = \beta_0 + \beta_1 \overline{H} + \beta_2 \overline{T}_{\max} \quad (15)$$

2.2.2. Predictive factorial regression model

Model 7: $$UVI_{max} = \beta_0 + \beta_1 \overline{H} + \beta_2 \overline{T}_{\max} + \beta_3 \overline{H} * \overline{T}_{\max} \quad (16)$$

2.2.3. Predictive response surface regression

Model 8: $$UVI_{max} = \beta_0 + \beta_1 \overline{H} + \beta_2 \overline{T}_{\max} + \beta_3 \overline{H}^2 + \beta_4 \overline{T}_{\max}{}^2 + \beta_5 \overline{H} * T_{\max} \quad (17)$$

Where, β*'s* are the coefficients of predictor variables, $\overline{H}$ and $\overline{T}_{\max}$ are considered more accurate effective for UVI_{max} forecasting results than other weather parameters.

2.3. Statistical evaluation

The performance of models will be judged by the statistical indicators such as Mean Bias Error (MBE), Root Mean Square Error (RMSE), Mean Absolute Percentage Error (MAPE), Mean Absolute Bias Error (MABE) and correlation coefficient (CC). These indicators are the ones that are applied most commonly in comparing the models of solar radiations. The test of MBE provides information on the long-term performance of the correlation by allowing a comparison of the actual deviation between estimated and measured values term by term (Al-

Hassany 2014, El-Mghouchi et al 2014). A positive MBE value means an over-estimation of the estimated values and a negative value means an under-estimation of the estimated values (Tian et al 2018). The RMSE is always positive; this test provides information on the short-term performance of the correlation by arranging a term by term comparison of the real differences between the estimated values and the measured values (Almorox 2011). RMSE is a good measure of precision. The MAPE is an overall measure of forecast accuracy (Almorox 2011), computed from the absolute mean relative difference between the global solar radiation of the measured data and those estimated by proposed model (El-Mghouchi et al 2014). The MABE gives the absolute value of bias error and it is a measure of the correlation goodness (Almorox 2011). It is recommended that a zero value for MBE is ideal while a low RMSE, MABE and MAPE are desirable. The correlation coefficient reflects the quality of the model; the higher CC (closed to 1), the highest model quality. The expression of each statistical indicator is given in the following forms (Almorox 2011).

$$MBE = \frac{\sum_{i=1}^{n}\left(\bar{H}_{i,estimated} - \bar{H}_{i,measured}\right)}{N},$$

$$MABE = \frac{\sum_{i=1}^{n}\left|\left(\bar{H}_{i,estimated} - \bar{H}_{i,measured}\right)\right|}{N},$$

$$RMSE = \sqrt{\frac{\sum_{i=1}^{n}\left((\bar{H}_{i,estimated} - \bar{H}_{i,measured}\right)^2}{N}}$$

$$CC = \frac{\sum_{i=1}^{n}(\bar{H}_{i,estimated} - \bar{H}_{estimated})(\bar{H}_{i,measured} - \bar{H}_{measured})}{\sqrt{\left(\sum_{i=1}^{n}(\bar{H}_{i,estimated} - \bar{H}_{estimated})^2\right)\left(\sum_{i=1}^{n}(\bar{H}_{i,measured} - \bar{H}_{measured})^2\right)}}$$

$$MAPE = \frac{1}{N}\sum_{i=1}^{n}\left|\frac{\bar{H}_{i,measured} - \bar{H}_{i,estimated}}{\bar{H}_{i,measured}}\right| * 100,$$ Where, N is Number of the observations.

3. RESULTS AND DISCUSSION

3.1. Empirical regression models and the prediction of monthly and daily average clear sky global solar radiation ($\bar{H}$ and H)

Various meteorological data are related to monthly average clear sky clearness index $\left(\bar{H}/\bar{H}_0\right)$. Empirical models are developed to estimate monthly and daily global radiation.

3.1.1. Empirical development regression models for estimating monthly average clear sky clearness index

Regression analysis of five models is employed to estimate the monthly average clear sky global solar radiation $(\bar{H})$. The empirical models are equations 1, 3, 5, 7 and 9. The following tables (1-4) show the coefficients of the empirical regression models to estimate $\bar{H}/\bar{H}_0$ for Sharm El-Sheikh, Aswan, Safaga and Cairo, respectively.

Table 1: The coefficients of the empirical regression estimation models for Sharm El-Sheikh

Regression Coefficients										
Models	b_0	b_1	b_2	b_3	b_4	b_5	b_6	b_7	b_8	b_9
Model 1	0.6857	0.42213	-0.00295	-0.01031						
Model 2	0.5374	0.47148	0.00192	-0.00825						
Model 3	1.331	0.70484	-0.00903	-0.11461	-0.0317	0.05895	0.00212			
Model 4	0.8843	-1.1197	2.8086	0.01045	0.00072	-0.08043				
Model 5	-43.9871	-28.810	57.884	0.17202	0.00531	8.20306	-0.16303	-0.27083	-4.2050	-0.0227

Table 2: The coefficients of the empirical regression estimation models for Aswan

Regression Coefficients										
Models	b_0	b_1	b_2	b_3	b_4	b_5	b_6	b_7	b_8	b_9
Model 1	0.5203	-0.01807	0.79727	-0.00353						
Model 2	0.0960	1.1528	0.01204	-0.02533						
Model 3	-1.8382	4.9737	-0.01216	0.17303	-0.04217	-0.3379	0.00294			
Model 4	0.2255	0.4241	1.8283	0.01918	0.00065	-0.0882				
Model 5	-35.6882	7.4866	39.6735	-0.05842	-0.0007	5.63753	-0.07642	-0.00571	-5.4167	0.0079

Table 3: The coefficients of the empirical regression estimation models for Safage

Regression Coefficients										
Models	b_0	b_1	b_2	b_3	b_4	b_5	b_6	b_7	b_8	b_9
Model 1	0.45123	0.14168	-0.00578	0.02337						
Model 2	0.77901	0.04318	-0.01659	0.01821						
Model 3	1.72539	2.60898	-0.05447	-0.19866	-0.06797	-0.02137	0.007618			
Model 4	1.210684	-2.12527	3.761624	3.06E-05	0.000929	-0.08158				
Model 5	-40.9489	-1.096	50.47372	-0.11439	-0.00118	6.99859	-0.11606	-0.00577	-6.0232	0.0142

Table 4: The coefficients of the empirical regression estimation models for Cairo

Regression Coefficients										
Models	b_0	b_1	b_2	b_3	b_4	b_5	b_6	b_7	b_8	b_9
Model 1	0.51251	0.25875	-0.00499	0.008132						
Model 2	0.62571	0.22771	-0.00937	0.007464						
Model 3	1.23308	-0.1230	-0.00957	-0.0800	-0.00707	0.07803	0.000735			
Model 4	0.73562	-0.3226	0.73023	-0.00517	9.6E-05	-0.00653				
Model 5	-44.0632	-10.8823	73.8287	-0.03741	-0.00086	7.73516	-0.08363	0.01431	-7.8058	0.00502

3.1.2. Statistical evaluation of the regression models

The results of the validation of the five models that estimate $\bar{H}$ for Sharm El-Sheikh, Aswan, Safaga and Cairo cities are shown in Table 5.

Table 5: Statistical indicators of accuracy for estimated regression models of Sharm El-Sheikh, Aswan, Safaga and Cairo

Sharm	MBE	RMSE	MAPE	MABE	CC	Aswan	MBE	RMSE	MAPE	MABE	CC
Model 1	**-9.8E-05**	0.0323	0.4216	0.0274	0.9998	Model 1	0.00032	0.1117	1.3882	0.0910	0.9967
Model 2	-0.00022	0.0336	0.4017	0.0269	0.9998	Model 2	**-0.00018**	0.0970	1.0706	0.0753	0.9975
Model 3	-0.00147	0.0312	0.3569	0.0240	0.9998	Model 3	-0.01081	**0.0680**	**0.8545**	**0.0577**	**0.9991**
Model 4	-0.0017	0.0290	0.3071	0.0207	0.9998	Model 4	0.00026	0.0854	0.9185	0.0645	0.9981
Model 5	0.00696	**0.0095**	**0.1205**	**0.0075**	**1.0000**	Model 5	0.06041	0.0797	1.0022	0.0667	0.9994
Safaga	**MBE**	**RMSE**	**MAPE**	**MABE**	**CC**	**Cairo**	**MBE**	**RMSE**	**MAPE**	**MABE**	**CC**
Model 1	**-0.00070**	0.0801	0.9261	0.0606	0.9982	Model 1	-0.00072	0.0560	0.7191	0.0451	0.9993
Model 2	0.00076	0.0795	0.8541	0.0576	0.9982	Model 2	**-0.00026**	0.0556	0.6587	0.0418	0.9993
Model 3	-0.00109	**0.0411**	**0.4367**	**0.0299**	**0.9996**	Model 3	0.00097	0.0549	0.6278	0.0401	0.9993
Model 4	-0.00153	0.0680	0.6782	0.0455	0.9987	Model 4	-0.00053	0.0547	0.6435	0.0412	0.9993
Model 5	-0.34037	0.3559	5.4666	0.3404	0.9998	Model 5	-0.01188	**0.0266**	**0.3063**	**0.0189**	**0.9999**

The obtained results of Sharm El-Sheikh and Cairo show that there are a remarkable agreement between the measured and predicted values using different regression models except Model 5 (the second-order polynomial regression model for three continuous predictor variable). This model gives high accurate results than other models according to the values of RMSE, MAPE, MABE and CC.

The suitable model for Aswan and Safaga cities is different than the suitatble one for Sharm El-Sheikh and Cairo. The interaction regression model for three continuous predictor variables (Model 3) fits Aswan and Safaga more than other regression models.

According to the value of MBE, Model 1 is appropriate for Sharm and Safaga as well as model 2 for Aswan and Cairo. But the value of MBE will not be taken into consideration, due to the disadvantage associated with MBE is that the errors of different signs may cancel each other. The smaller the MBE value, the better the model performs. However, some few values in the sum can produce a significant increase in the parameter. The MBE offers information regarding over-estimation or under-estimation of the estimated data;

low values of these mean errors are desirable, though it should be noted that over-estimation of an individual data element will cancel under-estimation in a separate observation (Almorox 2011).

3.1.3. The predictive model to estimate monthly average clear sky global solar radiation ($\bar{H}$)

From the previous analysis of models validation, the best model for estimating the $\bar{H}$ is the model that has three continuous predictor variables. The monthly average clear sky global solar radiation on a horizontal surface for each investigated city is:

For Sharm El-Sheikh, the response surface regression model (model 5, Table 1).

$$\bar{H}_{estimated} = (-43.9871 - 28.810C + 57.884C^2 + 0.17202T + 0.00531T^2 + 8.20306S - 0.16303S^2 - 0.27083C*T - 4.2050C*S - 0.0227T*S)* \bar{H}_0$$

For Aswan, the factorial regression model (model 3, Table 2).

$$\bar{H}_{estimated} = (-1.8382 + 4.9737C - 0.01216T + 0.17303S - 0.04217C*T - 0.3379C*S + 0.00294T*S)* \bar{H}_0$$

For Safaga, the factorial regression model (model 3, Table 3).

$$\bar{H}_{estimated} = (1.72539 + 2.60898C - 0.05447T - 0.19866S - 0.06797C*T - 0.02137C*S + 0.007618*S)* \bar{H}_0$$

For Cairo, the response surface regression model (model 5, Table 4).

$$\bar{H}_{estimated} = (-44.0632 - 10.8823C + 73.8287C^2 - 0.03741T - 0.000861T^2 + 7.73516S - 0.08363S^2 + 0.01431C*T - 7.8058C*S + 0.00502T*S)* \bar{H}_0$$

3.1.4. The results of $\bar{H}_{estimated}$ *of the best selected model in each city*

The values of $\bar{H}_0$, $\bar{H}/\bar{H}_0$, $\cos(\theta_{ZMT})$, T, S_0, and $\bar{H}_{estimated}$ are presented in Table 6-10. $\bar{H}_{estimated}$ is calculated form the best selected models (Model 5 for Sharm El-Sheikh & Cairo, and Model 3 for Aswan & Safaga (the equations given in the previous section).

Table 6: Monthly average meteorological data and clear sky global solar radiation for Sharm El-Sheikh using Model 5

MONTH	$\bar{H}_{measured}$ (KW/m²/day)	$\bar{H}_0$ (KW/m²/day)	$\bar{H}_{measured}/\bar{H}_0$	$cos(\theta_{ZMT})$	T	S_0	$\bar{H}_{estimated}/\bar{H}_0$	$\bar{H}_{estimated}$ (KW/m²/day)
JAN	**4.55**	6.2563	0.72727	0.47335	15.8	10.4467	0.7295	**4.564**
FEB	**5.58**	7.4431	0.74969	0.53653	16.5	11.0364	0.7507	**5.587**
MAR	**6.88**	8.9678	0.76719	0.61038	19.6	11.8304	0.7695	**6.901**
APR	**7.88**	10.308	0.76443	0.66447	24.0	12.6801	0.7652	**7.888**
MAY	**8.34**	11.089	0.75206	0.68588	27.7	13.3882	0.7534	**8.355**
JUN	**8.53**	11.349	0.75163	0.68930	30.0	13.7394	0.7518	**8.532**
JUL	**8.30**	11.187	0.74197	0.68823	31.3	13.5742	0.7426	**8.307**
AUG	**7.84**	10.556	0.74270	0.67545	31.4	12.9619	0.7424	**7.837**
SEPT	**6.98**	9.3964	0.74284	0.63373	30.1	12.1415	0.7429	**6.980**
OCT	**5.69**	7.8727	0.72275	0.56229	26.5	11.2938	0.7229	**5.692**
NOV	**4.72**	6.5046	0.72564	0.48926	21.8	10.5924	0.7265	**4.725**
DEC	**4.22**	5.8725	0.71861	0.45275	17.6	10.2591	0.7194	**4.225**

Table 7: Monthly average meteorological data and clear sky global solar radiation for Aswan using Model 3

MONTH	$\bar{H}_{measured}$ (KW/m²/day)	$\bar{H}_0$ (KW/m²/day)	$\bar{H}_{measured}/\bar{H}_0$	$cos(\theta_{ZMT})$	T	S_0	$\bar{H}_{estimated}/\bar{H}_0$	$\bar{H}_{estimated}$ (KW/m²/day)
JAN	**4.55**	6.8628	0.6630	0.50713	15.8	10.6916	0.66835	**4.587**
FEB	**5.77**	7.9584	0.7250	0.56584	16.8	11.1874	0.71999	**5.730**
MAR	**6.89**	9.3146	0.7397	0.63264	20.7	11.8569	0.74274	**6.918**
APR	**7.72**	10.4358	0.7398	0.67864	26.0	12.5737	0.73035	**7.622**
MAY	**7.86**	11.0251	0.7129	0.69370	29.9	13.1697	0.72340	**7.976**
JUN	**8.25**	11.1917	0.7372	0.69429	31.7	13.4644	0.72749	**8.142**
JUL	**8.00**	11.0731	0.7225	0.69452	32.5	13.3259	0.72113	**7.985**
AUG	**7.47**	10.6064	0.7043	0.68701	32.4	12.8112	0.70946	**7.525**
SEPT	**6.93**	9.6632	0.7172	0.65304	31.0	12.1194	0.70668	**6.829**
OCT	**5.79**	8.3337	0.6948	0.58941	27.3	11.4043	0.70027	**5.836**
NOV	**4.76**	7.0876	0.6716	0.52201	21.8	10.8139	0.66989	**4.748**
DEC	**4.22**	6.5004	0.6492	0.48779	17.4	10.5343	0.64359	**4.185** 4.18

Table 8: Monthly average meteorological data and clear sky global solar radiation for Safaga using Model 3

MONTH	$\bar{H}_{measured}$ (KW/m²/day)	$\bar{H}_0$ (KW/m²/day)	$\bar{H}_{measured}/\bar{H}_0$	$cos(\theta_{ZMT})$	T	S_0	$\bar{H}_{estimated}/\bar{H}_0$	$\bar{H}_{estimated}$ (KW/m²/day)
JAN	**4.41**	6.4436	0.68440	0.48391	14.7	10.5233	0.68274	**4.399**
FEB	**5.36**	7.6037	0.70492	0.54575	15.6	11.0836	0.70688	**5.375**
MAR	**6.42**	9.0780	0.70721	0.61747	19.3	11.8387	0.70760	**6.424**
APR	**7.20**	10.3519	0.69553	0.66912	24.3	12.6468	0.69021	**7.145**
MAY	**7.50**	11.0744	0.67724	0.68861	28.2	13.3198	0.68535	**7.590**
JUN	**7.91**	11.3049	0.69969	0.69117	30.5	13.6533	0.69275	**7.832**
JUL	**7.69**	11.1562	0.68930	0.69050	31.6	13.4965	0.69117	**7.711**
AUG	**7.10**	10.5760	0.67133	0.67931	31.5	12.9148	0.67344	**7.122**
SEPT	**6.23**	9.4823	0.65701	0.63993	29.9	12.1346	0.65316	**6.194**
OCT	**5.15**	8.0171	0.64238	0.57084	26.0	11.3283	0.64478	**5.169**
NOV	**4.33**	6.6850	0.64772	0.49951	20.8	10.6617	0.64696	**4.325**
DEC	**4.00**	6.0659	0.65942	0.46368	16.4	10.3453	0.65974	**4.002**

Table 9: Monthly average meteorological data and clear sky global solar radiation for Cairo using Model 5

MONTH	$\bar{H}_{measured}$ (KW/m²/day)	$\bar{H}_0$ (KW/m²/day)	$\bar{H}_{measured}/\bar{H}_0$	$cos(\theta_{ZMT})$	T	S_0	$\bar{H}_{estimated}/\bar{H}_0$	$\bar{H}_{estimated}$ (KW/m²/day)
JAN	**3.86**	5.9068	0.65349	0.45335	13.3	10.3004	0.65247	**3.854**
FEB	**4.72**	7.1401	0.66106	0.51895	13.6	10.9466	0.66164	**4.724**
MAR	**5.99**	8.7551	0.68417	0.59666	16.0	11.8147	0.68207	**5.972**
APR	**7.07**	10.2172	0.69197	0.65517	20.1	12.7433	0.69132	**7.063**
MAY	**7.46**	11.1074	0.67162	0.68006	23.4	13.5185	0.67114	**7.455**
JUN	**7.76**	11.4197	0.67953	0.68502	26.3	13.9037	0.67525	**7.711**
JUL	**7.35**	11.2325	0.65435	0.68325	28.2	13.7225	0.65592	**7.368**
AUG	**6.89**	10.5087	0.65565	0.66759	28.2	13.0517	0.64956	**6.826**
SEPT	**5.93**	9.22796	0.64261	0.62162	26.3	12.1546	0.64455	**5.948**
OCT	**4.76**	7.59878	0.62642	0.54590	22.8	11.2281	0.62252	**4.730**
NOV	**3.85**	6.16713	0.62428	0.46982	18.9	10.4603	0.62470	**3.853**
DEC	**3.49**	5.51261	0.63309	0.43207	14.8	10.0945	0.63201	**3.484**

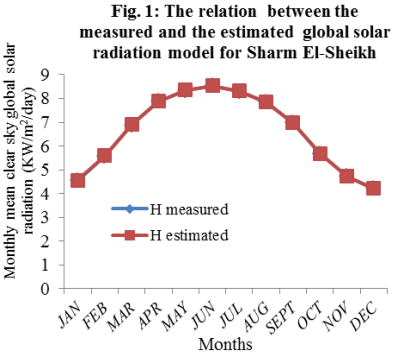

Fig. 1: The relation between the measured and the estimated global solar radiation model for Sharm El-Sheikh

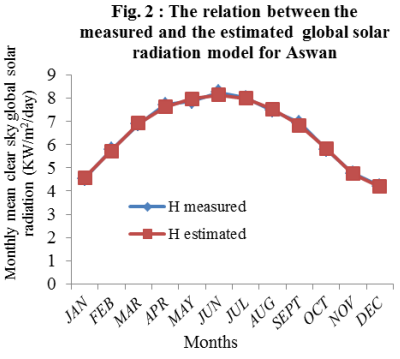

Fig. 2 : The relation between the measured and the estimated global solar radiation model for Aswan

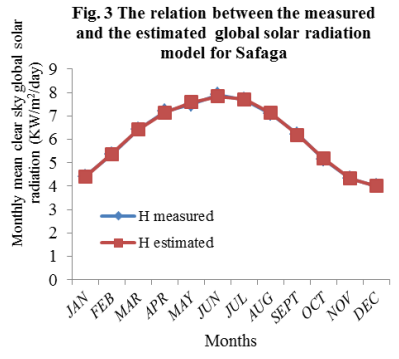

Fig. 3 The relation between the measured and the estimated global solar radiation model for Safaga

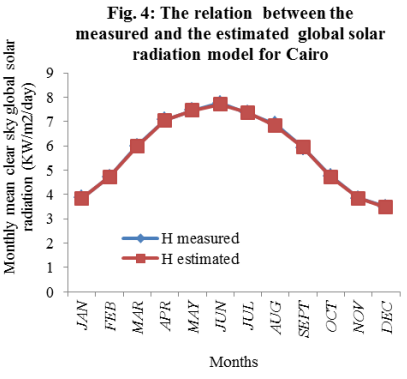

Fig. 4: The relation between the measured and the estimated global solar radiation model for Cairo

Figures 1-4 show the relation between the measured and predicted values of $\bar{H}$ using the suitable empirical development model for each city. It is clear from the figures that there is an excellent correlation and a perfect relationship exists between the measured and estimated

values of monthly average of clear sky global solar radiation. However, the estimated $\bar{H}$ overlaps the measured $\bar{H}$ in all months of the year. Figures 1-4 illustrate also that the values in the month range May-July belong to the maximum value for the global solar radiation. Moreover, the estimated high global solar radiation of the summer months is required for detailed study to get the maximum benefits of solar energy for the production of electric power.

3.1.5. Application of the predictive regression model for estimating daily clear sky global solar radiation on a horizontal surface (H) for Cairo city

To predict the daily clear sky global solar radiation (*H)* in Cairo, substitute the values of $\cos(\theta_{ZMT})$ and S_0, according to the corresponding month for the day that to be predicted, in the predictive response surface regression model (Model 5, Table 4). $\bar{T}$ is calculated from daily changing maximum and minimum temperature (eqn. 14). For example, to predict *H* of few days for some months, substitute the monthly values of S_0, $\cos(\theta_{ZMT})$ and $\bar{H}_0$ (from Table 9, for each month which corresponding that day to be predicted) in the following equation,

$$\bar{H}_{estimated} = (-44.0632 - 10.8823C + 73.8287C^2 - 0.03741T - 0.000861T^2 + 7.73516S - 0.08363S^2 + 0.01431C*T - 7.8058C*S + 0.00502T*S)* \bar{H}_0$$

The results are presented in Table 10.

Table 10: Some estimated values of daily clear sky global solar radiation in Cairo

Date	$\bar{H}_0$	$\cos(\theta_{ZMT})$	$\bar{T}$	S_0	$\bar{H}_{estimated} / \bar{H}_0$	$H_{estimated}$ KW/m²/ day
26-4-2018	10.2172	0.65517	(29+18)/2 = 23.50	12.743	0.68581	**7.007**
29-4-2018	10.2172	0.65517	(35+21.5)/2=28.25	12.743	0.64481	**6.588**
11-5-2018	11.1074	0.68006	(32+20)/2 = 26.00	13.519	0.66499	**7.386**
23-5-2018	11.1074	0.68006	(38.5+26.5)/2=32.5	13.519	0.59873	**6.650**
31-5-2018	11.1074	0.68006	(33+23)/2 = 28.00	13.519	0.65234	**7.246**
10-6-2018	11.4197	0.68502	(38.5+26)/2=32.25	13.904	0.62627	**7.152**
27-6-2018	11.4197	0.68502	(42.5+25)/2=33.75	13.904	0.60430	**6.901**
04-7-2018	11.2325	0.68325	(42+24)/2 = 33.00	13.723	0.60098	**6.751**
10-7-2018	11.2325	0.68325	(38+25)/2 = 31.50	13.723	0.62240	**6.991**

From Table 10, it should be noted that whenever the value of average day temperature increases, the value of global solar radiation decreases according to the corresponding days in the same month. That means, there is inversely relationship between the value of average temperature and the value of global solar radiation. The choice of the month range May-July is considered in this work because the effect of *UVI* is maximum. The prediction value of *H* is used for forecasting daily value of *UVI*.

3.2. Empirical regression models and the prediction of monthly and daily maximum ultraviolet index

In this section, three models are applied to estimate the monthly average UVI_{max} (eqns. 15-17) and are compared as attempt to deduce the best of one for each city. There is strong relationship between $\overline{H}$, $\overline{T}_{\max}$, as independent variable, and *UVI* , as dependant variable. That refers to try substituting many weather parameters for modeling UVI_{max}. Those model's predictors are found to give more accurate parameters for UVI_{max} forecasting results than other weather parameters.

3.2.1. The predictive model to estimate monthly average UVI_{max}

From the regression analysis and according to accuracy indicators, it has been found that the factorial regression model gives the best results in estimating monthly average UVI_{max} for Sharm El-Sheikh and Cairo. As well as, the response surface regression model gives the best results for Aswan and Safaga. The interaction and second-order polynomial regression models for two continuous predictor variables ($\overline{H}$ & $\overline{T}_{\max}$) are considered the suitable models for applications (Models 7 & 8). The best predictive model for estimation of monthly average UVI_{max} for each investigated city is :

For Sharm El-Sheikh,

$$UVI_{max} = -7.62325 + 1.9181\,\overline{H} + 0.25144\,\overline{T}_{\max} - 0.0196\,\overline{H} * \overline{T}_{\max}$$

For Aswan,

$$UVI_{max} = -11.7285 + 5.5139\ \bar{H} - 0.07192\ \bar{T}_{max} - 0.22392\ \bar{H}^2 + 0.00879\ \bar{T}_{max}^{\ 2} - 0.05541\ \bar{H} * T_{max}$$

For Safaga,

$$UVI_{max} = -27.0589 + 5.7864\ \bar{H} + 0.9889\ \bar{T}_{max} - 1.2353\ \bar{H}^2 - 0.04814\ \bar{T}_{max}^{\ 2} + 0.33922\ \bar{H} * T_{max}$$

For Cairo,

$$UVI_{max} = -5.2032 + 1.07451\ \bar{H} + 0.24131\ \bar{T}_{max} + 0.0011\ \bar{H} * \bar{T}_{max}$$

The results of the performance indicators show that the error rate for each predictive model is being reduced in varying proportions when compared with each other (Multiple Linear Regression (MLR) model, Factorial Regression (FR) model and response surface regression (RSR) model). The error rate of Sharm El-Sheikh predictive model is reduced by about 10% from MLR model and it has almost the same values of as those of RSR model. The error rate of Aswan predictive model is reduced by about 65% from MLR and 45% from FR models. The error rate of Safaga predictive model is reduced by about 65% from MLR and 50% from FR models. The error rate of Cairo predictive model is reduced by about 65% from MLR and 55% from RSR models.

Figures 5-8 show the relationship between the measured and estimated values of monthly average UVI_{max} using the suitable empirical developed model for each city. It is clear from the figures that there is an excellent correlation and a perfect relationship exists between the measured and estimated monthly average UVI_{max}.

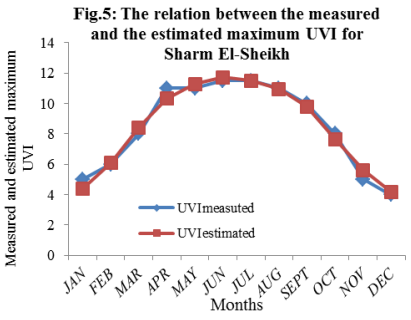

Fig.5: The relation between the measured and the estimated maximum UVI for Sharm El-Sheikh

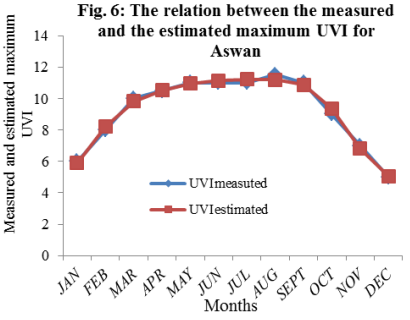

Fig. 6: The relation between the measured and the estimated maximum UVI for Aswan

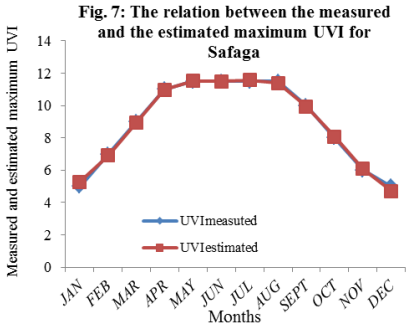

Fig. 7: The relation between the measured and the estimated maximum UVI for Safaga

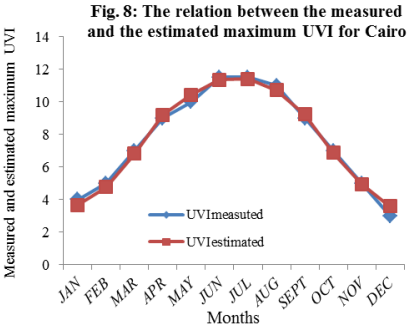

Fig. 8: The relation between the measured and the estimated maximum UVI for Cairo

The estimated value of daily UVI_{max} is calculated from monthly UVI_{max} estimation models, by substituting with the value of daily clear sky global solar radiation on a horizontal surface ($H_{estimated}$) and daily maximum temperature *(*$T_{\max}$*)*.

3.2.2. Application of the predictive regression model for estimating daily UVI_{max} for Cairo city

For example, to estimate the daily value of UVI_{max} of the same days in Table10, are has to substitute the values of $H_{estimated}$ and daily T_{max} (from Table 10) in the following interaction regression model (FR model):

$$UVI_{max} = -5.2032 + 1.07451\,\bar{H} + 0.24131\,\bar{T}_{\max} + 0.0011\,\bar{H} * \bar{T}_{\max}$$

The results of daily UVI_{max} values are presented in Table 11:

Table 11: Some estimated values of daily UVI_{max} in Cairo

Date	$H_{estimated}$	T_{max}	*Estimated* UVI_{max}
26-4-2018	7.007	29.0	**9.547**
29-4-2018	6.588	35.0	**10.575**
11-5-2018	7.386	32.0	**10.715**
23-5-2018	6.650	38.5	**11.514**
31-5-2018	7.246	33.0	**10.809**
10-6-2018	7.152	38.5	**12.075**
27-6-2018	6.901	42.5	**12.790**
04-7-2018	6.751	42.0	**12.498**
10-7-2018	6.991	38.0	**11.771**

From Table 11, it should be noted that whenever the value of global solar radiation decreases and maximum temperature increase, the

value of UVI_{max} increases according to each day in the same month. That means, there is inversely relationship between UVI_{max} and global solar radiation. In addition, there is a direct relationship between UVI_{max} and T_{max}..

3.2.3. The daily UV dose (DUVD)

It can be calculate as an integral of UV index over the daylight time as follows: $DUVD = \int_{T_0}^{T_{N+1}} UVI(t)dt$

Where, T_o is the sunrise time and T_{N+1} is the sunset time.

The calculations are performed again using the trapezoid rule that results in the following formula:

$$DUVD = \frac{1}{2}\sum_{j=0}^{N}(UVI_j + UVI_{j+1}) \cdot (T_{j+1} - T_j)$$

The daily *UV* dose is in *UV* Index hours (*UVI h*) if the units of T_j are in hours. To convert *UVI h* units to kJ/m^2, units that are commonly used to express *DUVD*, are has to multiply the result from the last equation by the factor: 0.09=25*3.6/1000 (Kiedron et al, 2007).

4. CONCLUSION

The statistical empirical estimation models of monthly and daily clear sky global radiation ($\bar{H}$ (for monthly) and H (for daily)) and maximum ultraviolet index (UVI_{max}) is constructed for states of Sharm El-Sheikh, Aswan, Safaga and Cairo. The empirical regression models are applied and compared. The applicable predictive regression models include multiple linear regression model, factorial regression model and response surface regression model. Three major predictor parameters are employed to estimate $\bar{H}$. The predictor variables are $T, \cos(\theta_{ZMT})$, S_0. The response variable is the variable to be predictable $\bar{H}/\bar{H}_0$. According to statistical evaluation, the second-order polynomial regression model for the three predictor variables (response surface regression model) is more applicable for Sharm El-Sheikh and Cairo than the other models. On the other hand, the interaction regression model for three predictor variables (factorial

regression model) fits Aswan and Safaga more than other regression models.

The empirical *H* developed model is considered as a simplified statistical approach because it depends on two monthly constant parameters (S_0 & $\cos(\theta_{ZMT})$), and one daily changeable parameter ($\overline{T}$) .The estimated high global solar radiation of the summer months is required for detailed study to get the maximum benefits of solar energy that to forecast UVI_{max} and for the production of electric power. The regression estimation models of UVI_{max} are based on two parameters. Precision of the developed forecasting model of monthly and daily UVI_{max} is based on maximum temperature ($\overline{T}_{\max}$ for monthly or T_{max} for daily) and accurate prediction of $\overline{H}$ or *H*. The global solar radiation and maximum temperature are considered more accurate and effective for UVI_{max} forecasting results than other meteorological parameters. The UVI_{max} results show that, the factorial regression model is the best for Sharm El-Sheikh and Cairo. Furthermore, the response surface regression model is more adequate for Aswan and Safaga than other models. The value of UVI_{max} increases with the increase in the value of maximum temperature, so that the increase in the UVI_{max} be linked to the low values of *H* for each day in the same month. The month range May-July (summer) was chosen in this work because the effect of *UVI* is maximum. There is an excellent correlation exists between the measured and predicted values for each of $\overline{H}/\overline{H}_0$ and UVI_{max}. Moreover, the predicted values of $\overline{H}/\overline{H}_0$ and UVI_{max} match the measured data in all months of the year.

REFERENCES

1. Adhikari K. R., Bhattarai B. K. and Gurung S., (2013); Estimation of Global Solar Radiation for Four Selected Sites in Nepal Using Sunshine Hours, Temperature and Relative Humidity Journal of Power and Energy Engineering, 1, pp. 1-9.
2. Al-Hassany Gh. S., (2014); Calculated the diffuse and direct parts of global solar radiation in Baghdad City for the Period (1983-2005) Depending on Clearness Index by Applying the Two

World Models of Liu–Jordan, Iraqi Journal of Physics, Vol. 12, No. 25, PP. 94-104.

3. Almorox J., (2011); Estimating global solar radiation from common meteorological data in Aranjuez, Spain, Turk J Phys, Vol. 35, pp. 53 – 64.
4. AmbientWeather.com - Smart Weather Stations; ***https://www.ambientweather.com/solarradiation.html.***
5. American Cancer Society; ***https://www.cancer.org/cancer/cancer-causes/radiation-exposure/uv-radiation/uv-radiation-what-is-uv.html.***
6. Augustine C. and Nnabuchi M. N., (2009); Empirical Models for the Correlation of Global Solar Radiation with Meteorological Data for Enugu, Nigeria, the Pacific Journal of Science and Technology Vol. 10, No. 1, pp. 693-700.
7. Chen J. L and Li G. Sh.,(2012); Estimation of Monthly Mean Solar Radiation from Air Temperature in Combination with Other Routinely Observed Meteorological Data in Yangtze River Basin in China, Journal of Meteorological Applications, Vol. 21, Issue 2, pp. 459-468.
8. Duffie J. A. and Beckman W. A. (2013); Solar Engineering of Thermal Processing, Fourth Edition, John Wiley & Sons, Inc.
9. El-Mghouchi Y., El Bouardi A. Choulli Z. and Ajzoul T., (2014); New Model to Estimate and Evaluate the Solar Radiation, International Journal of Sustainable Built Environment, Vol. 3, Issue 2, pp. 225-234.
10. El-Shanshoury G., El- Shanshoury H. and Abaza A., (2017); Health Effects of Low Level Ionizing Radiation Compared to Estimated UV index in Sharm El-Sheikh, Egypt, International Journal of Advanced Research (IJAR), Vol. 5, Issue 1, pp. 610-624.
11. Falayi E. O., Adepitan J. O. and Rabiu A. B.,(2008); Empirical Models for the Correlation of Global Solar Radiation with Meteorological Data for Iseyin, Nigeria International Journal of Physical Sciences Vol. 3. No. 9, pp. 210-216.
12. Habbib E. A., (2011), Empirical Models for Solar Radiation Estimation by Some Weather Data for Baghdad City, Al-Mustansiriya J. Sci, Vol. 22, No. 2, pp. 177-184.

13. Hatfield L. A., Hoffbeck R. W., Alexander B. H. and Carlin B. P., (2009); Spatiotemporal and Spatial Threshold Models for Relating UV Exposures and Skin Cancer in the Central United States. Comput. Stat. Data Anal., Vol. 53, No. 8, pp. 3001-3015. doi: 10.1016/j.csda.2008.10.013.
14. Hill T. and Lewicki P., (2007); STATISTICS: Methods and Applications. StatSoft, Tulsa, OK. StatSoft, Inc. (Electronic Statistics Textbook. Tulsa, OK: StatSoft., ***http://www.statsoft.com/textbook/.***
15. Ituen E. E., Esen N. U., Nwokolo S. C. and Udo E. G., (2012); Prediction of Global Solar Radiation Using Relative Humidity, Maximum Temperature and Sunshine Hours in Uyo, in the Niger Delta Region, Nigeria Advances in Applied Science Research, 2012, Vol. 3, No. 4, pp.1923-1937.
16. Kiedron P., Stierle S. and Lantz K., (2007); Instantaneous UV Index and Daily UV Dose Calculations, NOAA-EPA Brewer Network.1***www.esrl.noaa.gov/gmd/grad/neubrew/docs/UVindex.pdf.***
17. Miller A. C., Satyamitra M. and Kulkarni, S. (in press), "Late and Low Level Effects of Ionizing Radiation", Textbook of Military Medicine, Bender Press, Washington, DC [in press].
18. Namrataa K., Sharmab S. P. and Seksenaa S. B. L., (2016); Empirical Models for the Estimation of Global Solar Radiation with Sunshine Hours on Horizontal Surface for Jharkhand (India), Applied Solar Energy, Vol. 52, No. 3, pp. 164–172, Allerton Press, Inc.
19. NASA Surface Meteorology and Solar Energy–Choices, (2016); Atmospheric Science Data Center, Parameter Definition. ***https://eosweb.larc.nasa.gov/cgi-bin/sse/grid.cgi***.
20. Tian Z. , Perers B., Furbo S., Fan J., Deng J. and Dragsted J., (2018); A Comprehensive Approach for Modelling Horizontal Diffuse Radiation, Direct Normal Irradiance and Total Tilted Solar Radiation Based on Global Radiation under Danish Climate Conditions, Energies Journal, Vol. 11, 1315
21. Vanicek K., Frei Th., Litynska Z. and Schmalwieser A., (1999); UV- Index for the Public, A Guide for Publication and Interpretation of Solar UV Index Forecasts for the Public

Prepared by the Working Group 4 of the COST-713 Action "UVB Forecasting".

22. Weather2travel–climate guides, Egypt Climate and Weather, ***www.weather2travel.com/climate-guides/.***
23. Wiegant E., Van Geffen J., van Weele M., Van Der A. R. and Houweling S., (2016); Improving Satellite Based Estimations of UV Index and Dose and First Assessment of UV in A World-Avoided**.** Utrecht University, Master Thesis**,** KNMI Scientific Report WR-2016-01**.** 1-65.
24. Wikipedia, Ionizing Radiation; ***https://en.wikipedia.org/wiki/Ionizing_radiation.***